Predicting antibiotic resistance in complex protein targets using alchemical free energy methods

*Alice E Brankin[1] and Philip W Fowler[1,2]**

1. Nuffield Department of Medicine, John Radcliffe Hospital, University of Oxford, Oxford OX3 9DU, UK

2. National Institute of Health Research Oxford Biomedical Research Centre, John Radcliffe Hospital, Headley Way, Oxford OX3 9DU, UK

KEYWORDS free energy calculations; molecular dynamics; tuberculosis; antimicrobial resistance

ABSTRACT

Multi-drug resistant *Mycobacterium tuberculosis* requires a complex antibiotic treatment program and poses a major threat to tuberculosis (TB) treatment outcomes. Resistance is mostly conferred by chromosomal single nucleotide polymorphisms, many of which are well characterized and catalogued. However, not all mutations have been mapped and novel mutations can emerge. Methods able to quickly predict the effects of such mutations are needed to complement the existing catalogues, thereby permitting the prescription of effective treatment for patients and preventing the further spread of resistant strains. Relative binding free energy (RBFE) calculations can rapidly predict the effects of mutations, but this approach has not been tested on large, complex proteins. We use RBFE calculations to predict the effects of seven *M. tuberculosis* RNA polymerase mutations on rifampicin susceptibility and five *M. tuberculosis* DNA gyrase mutations on moxifloxacin susceptibility. These mutations encompass a range of amino acid substitutions with known effects and include large steric perturbations and charged moieties. We find that moderate numbers (n=3-15) of short RBFE calculations can predict resistance in cases where the mutation results in a large change in the binding free energy, but that the method lacks discrimination in cases with either a small change in energy or that involve charged amino acids, due to the associated large magnitude of error. We investigate how this error may be decreased by analyzing the sources of error and the distributions of repeated measurements from the different components of the RBFE calculations.

INTRODUCTION

Tuberculosis is a difficult disease to treat; the standard regimen is four antibiotics, rifampicin, isoniazid, pyrazinamide and ethambutol, for six months. An infection that is resistant to both rifampicin and isoniazid is called multi-drug resistant tuberculosis (MDR-TB) and the treatment regimen recommended by the World Health Organization (WHO) is complex but always includes levofloxacin or moxifloxacin, which are fluoroquinolones[1].

Rifampicin acts by binding to the β-subunit of the RNA polymerase (RNAP, encoded by the *rpoB* gene), preventing the extension of the RNA (Fig. 1a). The most common resistance-conferring mutation is *rpoB* S450L, however a wide range of mutations have been observed clinically[2-5]. The majority of these are found in amino acids 428 to 452 which pack against the drug (usually known as the *"rifampicin resistance determining region"* or RRDR), enabling the development of nucleic acid amplification tests, such as the Cepheid GeneXpert MTB/RIF system which is endorsed by the WHO for diagnosis of MDR-TB[6,7]. Not all non-synonymous mutations in the RRDR, however, confer resistance, for example *rpoB* L443F[5]. Nor does resistance arise purely within the RRDR: *rpoB* I491F and V170F are proximal to S450L and the former was suspected to be behind an outbreak of MDR-TB in Eswatini since it is not detected by GeneXpert[8].

The fluoroquinolones target the DNA gyrase (DNAG), a tetrameric enzyme which unwinds DNA by forming and re-ligating double stranded DNA breaks prior to transcription and replication (Fig. 1b). Specifically, two fluoroquinolone molecules intercalate into DNA breaks and bind specific *gyrA* residues via a coordinated Mg^{2+} ion. This stabilizes DNA-DNA gyrase covalent linkages and prevents re-ligation of DNA double stranded breaks.

The most common DNA gyrase mutations found in MDR-TB samples are *gyrA* D94G and *gyrA* A90V and these mutations are strongly associated with fluoroquinolone resistance[2, 3, 9-12]. These residues are part of the *gyrA "quinolone resistance determining region"* (QRDR), defined as *gyrA* codons 74 to 113[13]. However, again, not all mutations in this region confer resistance, leading to false positive resistance results in genotypic assays[14]. Rarely seen DNA gyrase mutations in *gyrB* are also associated with fluoroquinolone resistance, and a *gyrB* QRDR from residues 461 to 501 has also been proposed[15]. The residues of the two QRDR regions make up the fluoroquinolone binding pocket, and *gyrB* A642P is the only mutation significantly associated with an increase in minimum inhibitory concentration (MIC) to fluoroquinolones that was found outside this region[9].

We assume that mutations cause resistance by reducing the affinity of an antibiotic ligand for its target. Since we are only interested in whether a mutation increases or decreases the antibiotic's affinity for the target, the difference in binding free energy ($\Delta\Delta G$) between the wild type and mutant systems is calculated. This can be achieved by employing relative binding free energy (RBFE) methods, whereby a wild type amino acid is transmuted into the mutant along a non-physical pathway defined by a progress coordinate, $0 \leq \lambda \leq 1$. For equilibrium-based methods, a series of short molecular dynamics (MD) simulations are performed at fixed values of λ and the resulting ΔG values are related to the difference in binding free energy via a thermodynamic cycle (Fig. 2). This approach has been shown to successfully predict if mutations in a relatively small protein, *S. aureus* DHFR[16, 17] (157 residues), confer resistance to trimethoprim, an antibiotic used to treat urinary-tract infections. In this paper we shall apply the same approach to two much larger protein complexes, the RNA polymerase (4,671 residues) and the DNA gyrase cleavage complex (1,473 residues), to assess how well we can predict the effect of seven and five mutations on the action of rifampicin and moxifloxacin, respectively.

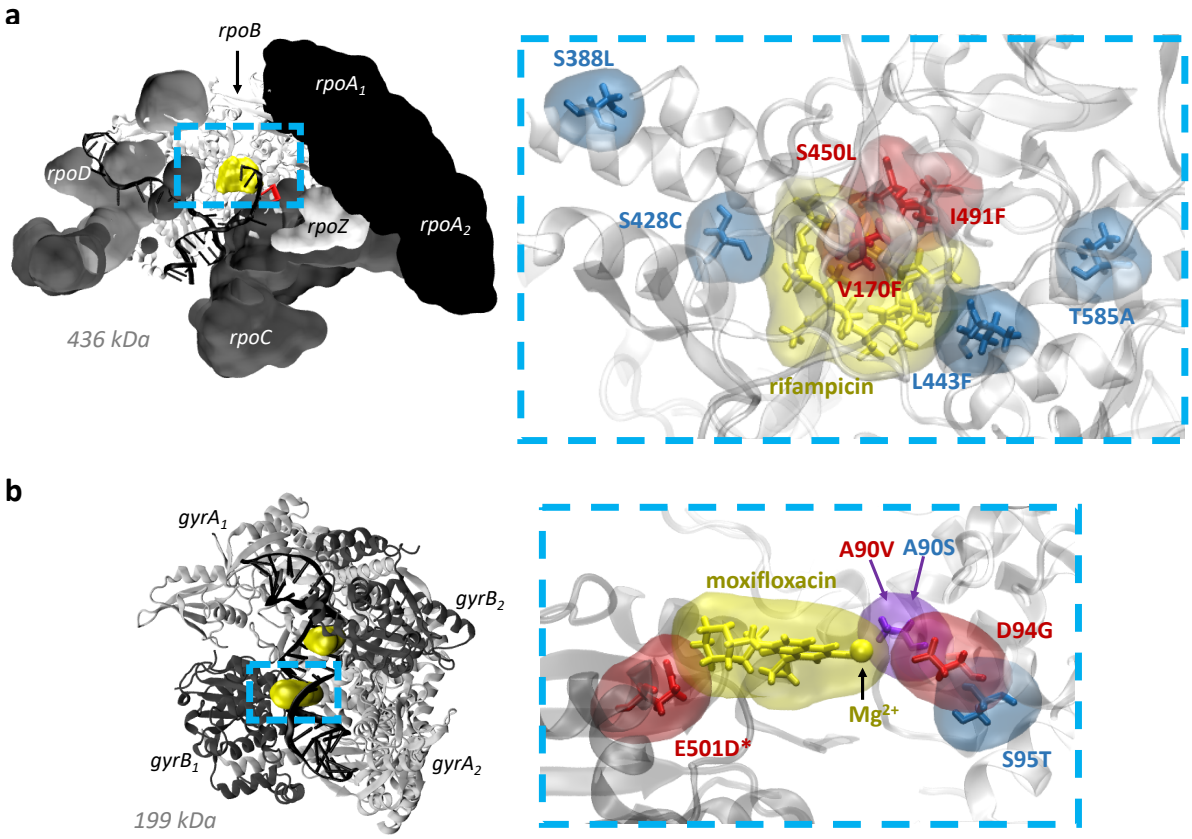

Figure 1. Structures of *M. tuberculosis* (a) RNA polymerase (RNAP)[18] and (b) DNA gyrase (DNAG)[19] cleavage complex, showing the selected clinical mutations associated with antibiotic resistance and susceptibility relative to the antibiotic binding sites. For clarity, RNAP subunits (excluding *rpoB*) are shown in surface view and nucleic acids are hidden in close-up visualisations. Resistance-conferring mutations are drawn in red, those associated with susceptibility blue and those residues where different mutations confer different resistance phenotypes purple. An asterisk (*) indicates a *gyrB* mutation.

METHODS

RNA polymerase and DNA gyrase system setup. The structure of the *M. tuberculosis* RNA polymerase (PDB:5UH6)[18], including a 14-base stretch of DNA, 2 RNA nucleotides, 2 zinc ions, a magnesium ion and a bound rifampicin molecule, was solvated with 114,838 waters and 127 sodium ions – the latter to ensure electrical neutrality – creating a cubic simulation unit cell of initial dimensions 20.1 x 15.2 x 13.1 nm. The flexible loop region of each gyrB protein that were not resolved in the structure of the *M. tuberculosis* DNA gyrase cleavage complex (PDB:5BS8)[19] were modelled in using the ModLoop server[20]. This structure, including the 19-base stretch of DNA, 4 Mg^{2+} ions, 2 bound moxifloxacin molecules and 403 crystal waters was placed in a rhombic dodecahedron unit cell with dimensions 13.8 x 13.8 x 9.8 x 0.0 x 0.0 x 0.0 x 0.0 x 6.9 x 6.9 nm. The unit cell was solvated with 59,895 waters, 175 Na^{+} and 112 Cl^{-} ions providing electrical neutrality and a 100mM salt concentration. The generalized AMBER and AMBER ff99SB-idln forcefields were used throughout[21]. To facilitate the covalent bond between *gyrA* Tyr129 and the phosphate backbone of DNA by GROMACS, two modified amino acids (TYX and TYY) were created. These 'hybrid' amino acids contained the parameters for Tyr, excluding the hydroxyl hydrogen, all nucleotides in the covalently bound DNA chain and the covalent bond between the Tyr hydroxyl oxygen and the corresponding DNA backbone phosphorus atom. The PDB file order and residue naming was adjusted to reflect the modified amino acids. The system was left with a non-integer charge due to the exclusion of the hydrogen atom from Tyr, so a solvent chloride ion was modified to provide a balancing charge.

The energies of the resulting RNA polymerase and DNA gyrase unit cells of 396,776 atoms and 205,883 atoms, respectively, were then minimized by GROMACS[22] 2016.3 and 2018.2 respectively, using a steepest descent algorithm for 1,000 steps before being gradually warmed

from 100 K to 310 K over 500 ps. For comparison, the DHFR unit cell only contained 27,115 atoms[16, 17]. The resulting structure and velocities were used to seed three RNAP and five DNAG equilibration simulations, each 50 ns long. The temperature was maintained at 310K using a Langevin thermostat with a time constant of 2 ps. An isotropic Parrinello-Rahman barostat with a 1 ps time constant and a compressibility of 4.46 x 10^{-5} bar^{-1} was applied to keep the pressure at 1 bar. Electrostatic forces were calculated using the particle mesh Ewald algorithm with a real space cutoff of 1.2 nm whilst van der Waals forces were only calculated between atoms less than 1.2 nm apart with a switching function applied from 0.9 nm. The lengths of all bonds involving a hydrogen were constrained using LINCS[23], permitting a timestep of 2 fs. For DNA gyrase, to prevent the moxifloxacin coordinated Mg^{2+} from dissociating from moxifloxacin, we used a harmonic distance restraint of sufficient strength (100,000 kJ mol^{-1} nm^{-2}) to maintain the distance observed in the crystal structure (0.209 nm) throughout all simulations, lower values were not sufficient. A series of assumed independent structures were obtained by saving the coordinates of the system every 10 ns from each of three RNAP equilibration simulations and each of five DNAG equilibration simulations.

Mutations were then introduced into each of these structures using pmx[24]. To reduce the likelihood of clashes between the 'new' sidechain and the remainder of the protein (i.e. in simulations with $\lambda \sim 1$) we then applied a short Alchembed procedure[25] to each structure – this involved a 1,000 step simulation where λ was increased from 0 to 1 using a soft-core van der Waals potential. This created a pool of presumed independent mutated structures that could be used to seed alchemical thermodynamic integration simulations.

Following best practice[26], the free energies (Fig. 2) required to remove the electrical charge on the perturbing atoms (ΔG_{qoff}), transmute the van der Waals parameters (ΔG_{vdW}) and recharge the

remaining atoms (ΔG_{qon}) were separately calculated using GROMACS 2016.3 for RNAP and 2019.1 for DNAG. Each calculation required eight simulations at equally spaced values of the progress parameter, λ. To accelerate convergence, 10,000 replica exchanges were attempted between neighboring λ-simulations every 1,000 timesteps. The process was repeated for both apo and complexed forms of either the RNAP or DNAG, thereby resulting in six independent free energies (Fig. 2). The timestep was reduced from 2 fs to 1 fs and LINCS constraints were removed for the vdW transitions for all DNA gyrase mutations and the qon transition of *gyrA* D94G to prevent crashing. To ensure the drug remained bound, a harmonic distance-based potential with spring constant 1,000 kJ mol^{-1} nm^{-2} was applied between the centers of mass of the drug and the RNAP beta subunit. Two additional free energies describing the cost of removing this restraint (Fig. 2) were then also calculated.

Calculation of errors. In previous studies of *S. aureus* DHFR[16, 17] all alchemical free energies were repeated the same number of times which, since *n* values of the final difference in binding free energy ($\Delta\Delta G$) were then obtained, simplified the calculation of errors. Both simulation unit cells studied here were over an order of magnitude larger and we therefore instead calculated errors at the level of an individual alchemical free energy (e.g. ΔG_{vdW}), with the final error in $\Delta\Delta G$ estimated by adding these in quadrature. Throughout a 95% confidence limit was estimated by multiplying the standard error by the appropriate *t*-statistic. We arbitrarily decided that at least three independent values of each alchemical free energy would be calculated, and then additional repeats would be run with the aim of reducing the magnitude of the overall 95% confidence limit to less than 1 kcal/mol. Achieving the latter was not always possible even when large numbers of repeats were run ($n \geq 10$, see Supplementary Information).

Simulations run. Overall, 241 alchemical free energies, each requiring 8x λ simulations 0.5 ns long, were calculated for the RNA polymerase allowing the six mutations to be studied. When the equilibration simulations are included, this is a total of 1.11 μs of molecular dynamics simulations. To study the five DNA gyrase mutations, a total of 231 alchemical free energies were calculated (8x λ simulations 0.5 ns long) and including equilibration simulations, a total of 1.17 μs of molecular dynamics simulations were initially performed. As described later, for DNA gyrase, nine calculations were extended to 5 ns which increased the total molecular dynamics performed to 1.49 μs. To avoid equilibration effects, the first 0.25 ns of each λ simulation was discarded.

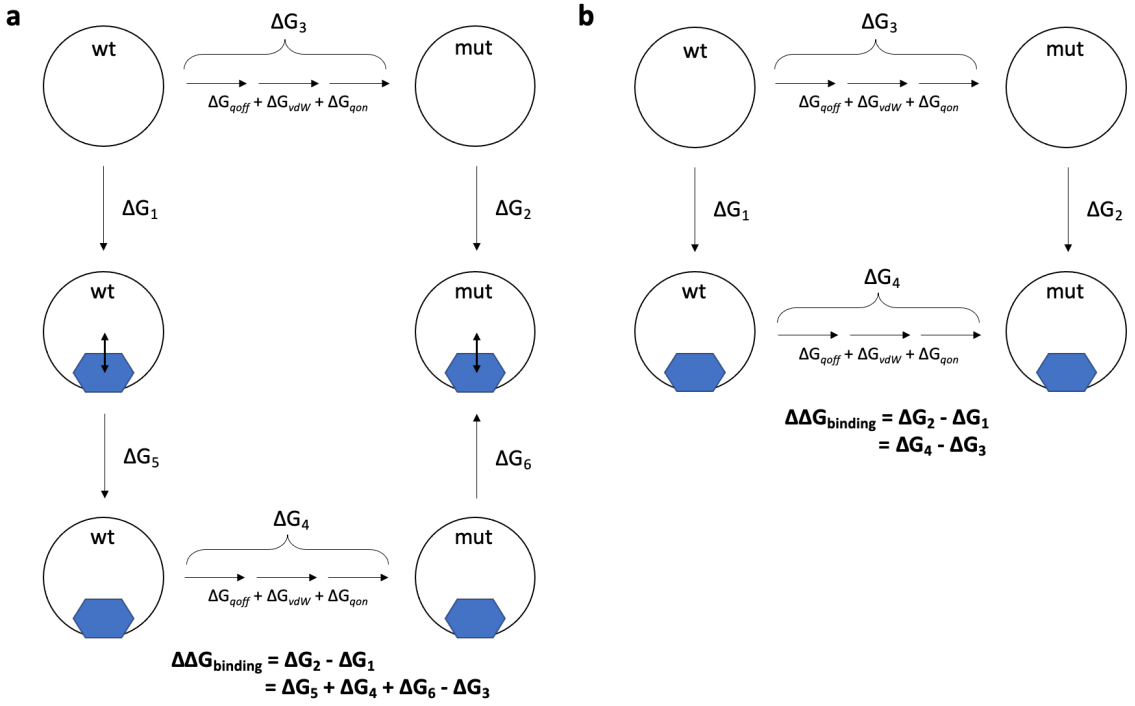

Figure 2. Free energy cycles for (a) rifampicin binding RNAP and (b) moxifloxacin binding DNAG gyrase cleavage complex. The subscripts qoff, vdW and qon describe the process of first removing the electrical charge from atoms being perturbed, followed by transforming their van

der Waals parameter, before finally recharging the atoms being perturbed. Double headed arrows represent the restraint used to prevent rifampicin from leaving the binding pocket. In all cases we are making use of the fact that free energy is a state function and therefore we can write the difference binding free energy ($\Delta\Delta G_{binding}$) as a sum of so-called alchemical free energies (e.g. ΔG_4 - ΔG_3).

RESULTS

Selecting the mutations studied

To test the ability of RBFE to predict antibiotic resistance we selected a small number of mutations in the RNAP and DNAG that confer resistance; to act as negative controls we added several more mutations known to have no clinical effect. We chose to test the most common resistance-conferring mutations for each drug. For RNAP this is S450L in the RRDR of *rpoB* and for the DNA gyrase these are A90V and D94G in the QRDR of *gyrA* (Fig. 1). D94G is a robust test of RBFE as the mutation involves a significant change in amino acid properties and electrical charge. For rifampicin we also selected V170F and I491F in *rpoB* which both confer resistance, are proximal to both S450L and the antibiotic binding site, but are not in the RRDR (Fig. 1a). I491F is one of the so-called "disputed" mutations which either have variable or borderline rifampicin minimum inhibitory concentrations[12, 27]. For moxifloxacin we also tested E501D in *gyrB*[12] which is close to the antibiotic binding site but not in the *gyrA* QRDR (Fig. 1b).

When choosing negative controls, we prioritised mutations that were observed multiple times in clinical samples, are close to the drug binding site and do not involve a charge change or a proline residue. For the RNAP, L443F was selected since it lies within the RRDR and is close to the rifampicin binding site yet does not confer resistance[11] and therefore is a good negative control (Fig. 1a). We also selected S388L and T585A which are further from the binding site and are seen in clinical samples. Finally, we choose an amino acid (Ser428) at which non-synonymous mutations are expected to confer resistance, since it lies in the RRDR, but for which no firm statistical association has been made, and choose a mutation (S428C) which minimally chemically perturbs the sidechain. We expect this to not confer resistance, since it has not been observed

clinically and the sidechain points away from the drug and is therefore a good, if somewhat artificial, negative control.

For the DNA gyrase negative controls, we chose *gyrA* S95T (Fig. 1b) since it is very common – it is found in almost all samples except the H37Rv reference genome - and is within the QRDR. Testing different mutations at the same position which have different effects is a particularly stringent test of the ability of RBFE methods to predict antibiotic resistance. We therefore also tested the *gyrA* A90S mutation (Fig. 1b) – this is not seen clinically but a serine is present at the equivalent position in the DNA gyrase of other bacterial species and is suggested to help stabilise the gyrase-fluoroquinolone complex via participation in water-ion bridging interactions with the drug coordinated Mg^{2+}. *M. tuberculosis* has some innate immunity to fluoroquinolones which has been suggested is due to the alanine at this position[19]. The *gyrA* A90S mutation is therefore expected to strengthen the binding of moxifloxacin, thereby conferring *hyper-susceptibility*.

Predictions

The simplest approach is to assume that a positive value of the change in binding free energy of the antibiotic ($\Delta\Delta G < 0$) indicates that the antibiotic binds less well to the target following the mutation and therefore would be predicted to confer resistance to that drug. Clinically, however, a sample is categorized as 'resistant' if its minimum inhibitory concentration (MIC) is greater than a critical concentration, often the epidemiological cutoff value (ECOFF/ECV), which is defined as the MIC of the 99th percentile of a collection of phenotypically-wildtype samples. Such thresholds for both drugs were derived using published ECOFF/ECV values[28] as described previously[17].

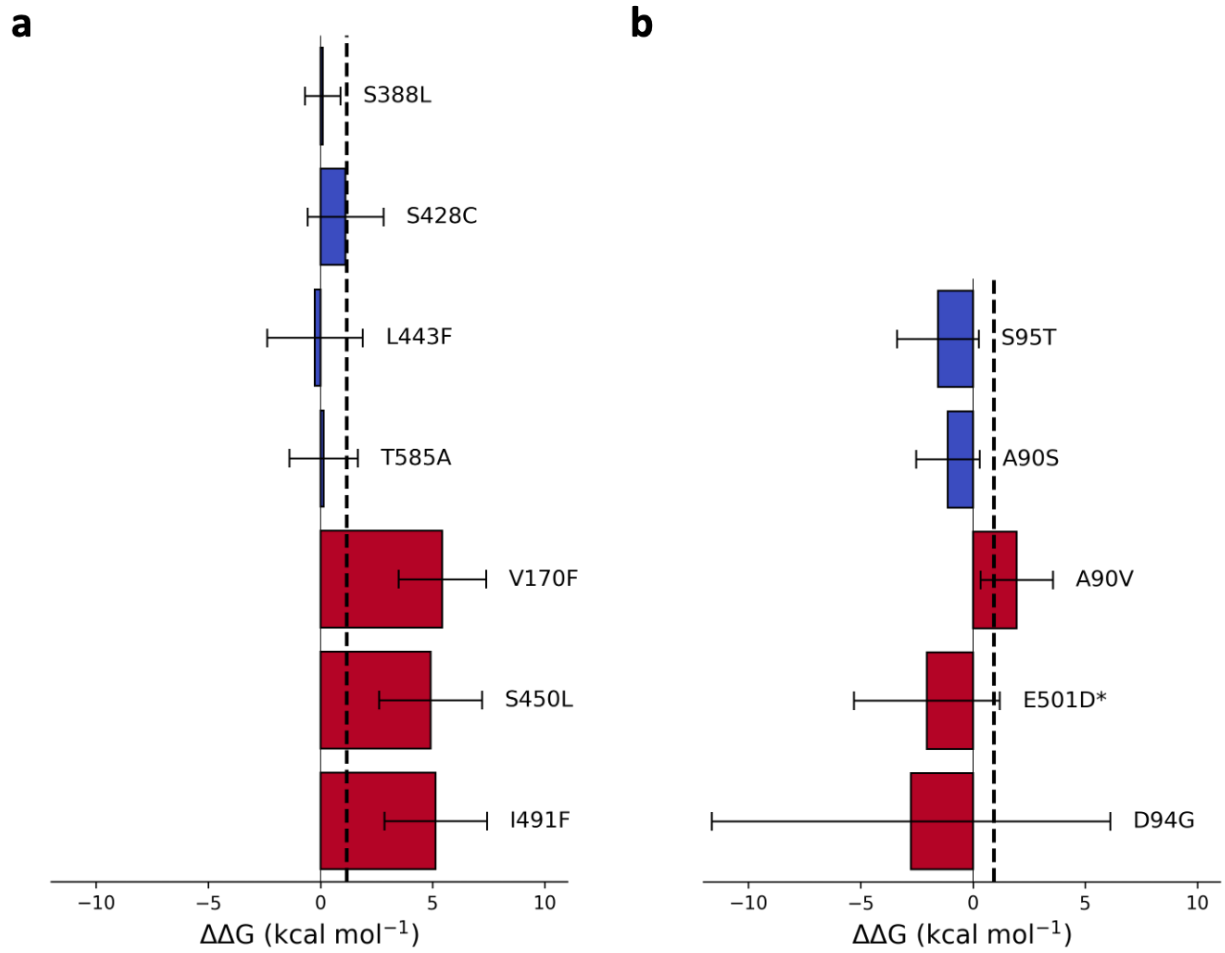

Figure 3. The calculated effect of the listed mutations on the binding free energy of (a) rifampicin to RNAP and (b) moxifloxacin to DNA gyrase. Dotted lines represent the value of ΔΔG equivalent to the epidemiological cutoff value for (a) rifampicin and (b) moxifloxacin; above this value an *M. tuberculosis* isolate would be considered clinically resistant. Bars represent the mean ΔΔG for each susceptible (blue) and resistant (red) mutation compared to the wild-type protein and 95% confidence limits are shown, calculated using the appropriate *t*-statistic. An asterisk (*) indicates a *gyrB* mutation.

Table 1. Summary of free energy calculations for RNAP and DNAG mutations

Protein	Mutation	Expectation	ΔΔG (kcal mol^{-1})	N [1]	N_{min} [2]	N_{max} [2]
RNAP	S388L	Susceptible	0.1 + 0.8	18	3	3
	S428C	Susceptible	1.1 ± 1.7	21	3	5
	L443F	Susceptible	-0.2 ± 2.1	28	3	8
	T585A	Susceptible	0.2 ± 1.5	20	3	4
	V170F	Resistant	5.4 ± 1.9	37	3	13
	S450L	Resistant	4.9 ± 2.3	49	4	13
	I491F	Resistant	5.1 ± 2.3	22	3	5
DNAG	S95T	Susceptible	-1.6 ± 1.8	50	5	15
	A90S	Hyper-susceptible	-1.1 ± 1.4	33	5	8
	A90V	Resistant	2.0 ± 1.6	44	4	15
	E501D*	Resistant	-2.0 ± 3.2	59	9	10
	D94G	Resistant	-2.8 ± 8.9	45	4	10

[1] N is the total number of free energy calculations used to calculate the ΔΔG, excluding the *rpoB* restraints as their contributions were negligible (see Supplementary Information) [2] N_{min} and N_{max} list the minimum and maximum number of repeat calculations used for apo or drug-bound de-charging (ΔG_{qoff}), van der Waals (ΔG_{vdW}) or re-charging (ΔG_{qon}) transitions, respectively (Figure 2). * indicates a *gyrB* mutation.

Three independent values of ΔΔG were first calculated. Each value of ΔΔG required the calculation of 6-8 alchemical free energies (Fig. 1, Methods). Repeats of the alchemical free energy components exhibiting the greatest variation were then run to efficiently reduce the confidence limits of the prediction as described in the Methods. First let us consider the overall values of ΔΔG and whether successful predictions can be made.

For rifampicin, only one of the four negative controls (S388L) was correctly predicted to have no effect on the action of rifampicin (Fig. 3a); since the confidence limits of S428C, L443F and T585A all bracket the ECOFF threshold no definite prediction could be made for these mutations. Clinically the method as implemented would therefore return an 'Unknown' phenotype for these

mutations. All three rifampicin-resistance conferring mutations, including the disputed mutation I491F, not only have positive values of ΔΔG but also lie above the clinical threshold derived from the ECOFF/ECV. These mutations are therefore correctly predicted to confer resistance to rifampicin.

Both moxifloxacin negative controls (*gyrA* S95T & A90S) were correctly predicted to not affect the binding of moxifloxacin to the DNA gyrase. Although hyper-susceptibility is expected for A90S, the magnitude of the confidence limits prevents us drawing any conclusions. No definite prediction could be made for any of the three mutations associated with moxifloxacin resistance since the confidence limits of all three mutations straddled the clinical threshold. Unlike the RNA polymerase, two of the mutations to the DNA gyrase involved charged residues (*gyrB* E501D & *gyrA* D94G) and not surprisingly these had the largest estimated errors.

To see how our ΔΔG values compared with clinical resistance measurements, we calculated an estimated 'expected ΔΔG' corresponding to the geometric mean of MICs associated with each of the resistance conferring mutations, using previously described methods[17]. However, the errors in both the 'expected ΔΔG' and the ΔΔG values calculated by RBFE were too large to enable us to draw any conclusions about how well the values compare with one another (Fig. S1).

The magnitudes of the estimated errors prevented us from making a definite classification in six of the 12 mutations studied. One hypothesis is that the larger the alchemical perturbation, the larger the magnitude of error. We therefore examined whether there was a correlation between the number of atoms where the atom type was perturbed during the alchemical transition and the

magnitude of error in calculated ΔΔG values (Fig. S2). There was a weak positive correlation for both RNAP and DNAG mutations, suggesting that whilst this does play a role, it is not the main driver behind the large errors observed here.

To further examine what is driving the magnitudes and confidence limits of the individual ΔΔG values in Fig. 3, we analysed the alchemical free energy components from the de-charging (ΔG_{qoff}), van der Waals (ΔG_{vdW}) and re-charging (ΔG_{qon}) transitions (Fig. 2) for both apo and drug-bound legs of the free energy calculations (Fig. 4). As expected, for both the RNA polymerase and the DNA gyrase, there were no significant differences for the negative control mutations between the mean apo and drug-bound values of ΔG_{qoff}, ΔG_{vdW} and ΔG_{qon} and the estimated error is generally low.

For all three resistance-conferring mutations in *rpoB* the value of ΔG_{vdW} when rifampicin is bound is significantly greater than the same transition for the apo protein and it is this that is mainly driving the positive value of ΔΔG. The difference between the apo- and rifampicin-bound vdW transitions for V170F, S450L and I491F are 4.6, 5.6 and 5.3 kcal/mol, respectively. Since all three of these mutations involve the introduction of a larger sidechain that is oriented towards the bound drug, this is consistent with resistance arising primarily through steric hindrance of the rifampicin binding site. For comparison, despite a similar number of atoms being perturbed, there was no difference in the apo- and drug-bound values of ΔG_{vdW} for the susceptible mutation *rpoB* L443F, which is also in the RRDR (Fig. 1a) and, whilst this also involves the introduction of a larger sidechain, in the crystal structure this is directed away from rifampicin. Differences in ΔG_{vdW}

between the apo- and complexed DNA gyrase also appear mainly responsible for the positive value of ΔΔG for *gyrA* A90V, however the net effect is reduced.

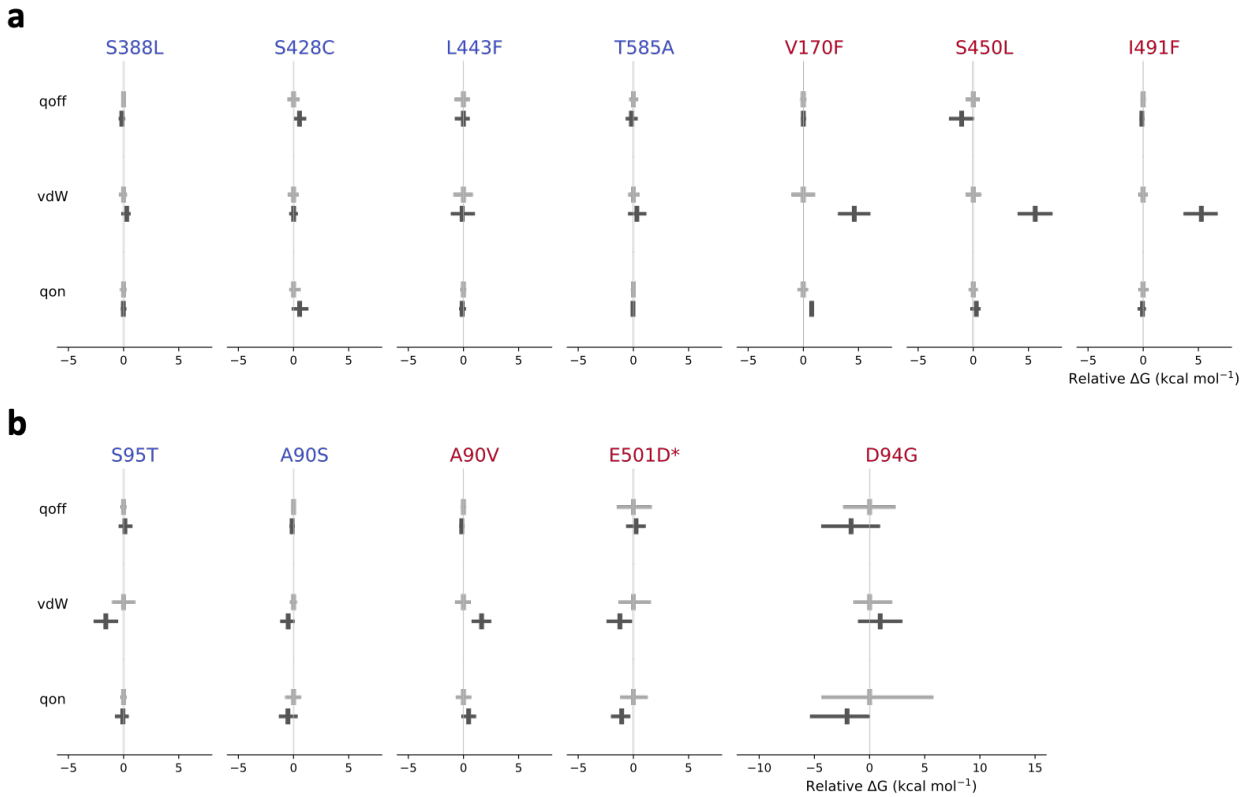

Figure 4. Apo (light grey) and drug-bound (dark grey) free energy calculations for (a) RNAP and (b) DNA gyrase mutations for de-charging (qoff), van der Waals (vdW), and re-charging (qon) transitions. All results are normalized to the mean of the calculations for the apo leg for each transition for each mutation. Mean values are denoted by a cross and the error bars describe the 95% confidence limits, calculated from the SEM using the appropriate *t*-statistic. The free energy cost of removing the restraints for rifampicin is not shown since for all mutations it is negligible, indicating that restraints were likely not required to keep the drug in the binding site. An asterisk (*) indicates a *gyrB* mutation.

Hence the variation in ΔΔG arises mainly from the apo and complexed values of ΔG_{vdW} – the notable exceptions being *gyrB* E501D and *gyrA* D94G. This is despite our efforts to minimize the overall error by running up to 4x the number of repeats for those transitions (Table 1) to reduce their individual estimated errors. For *gyrB* E501D and *gyrA* D94G all three transitions contribute significant error, which since they add in quadrature, leads to a large overall error in ΔΔG. This is not surprising since both mutations involve turning off (and on) electrical charge and D94G involves a net charge change that must be compensated for elsewhere in the system. To investigate how far we might reduce the errors, let us now consider the individual values of ΔG_{qoff}, ΔG_{vdW} and ΔG_{qon} (Figure 5).

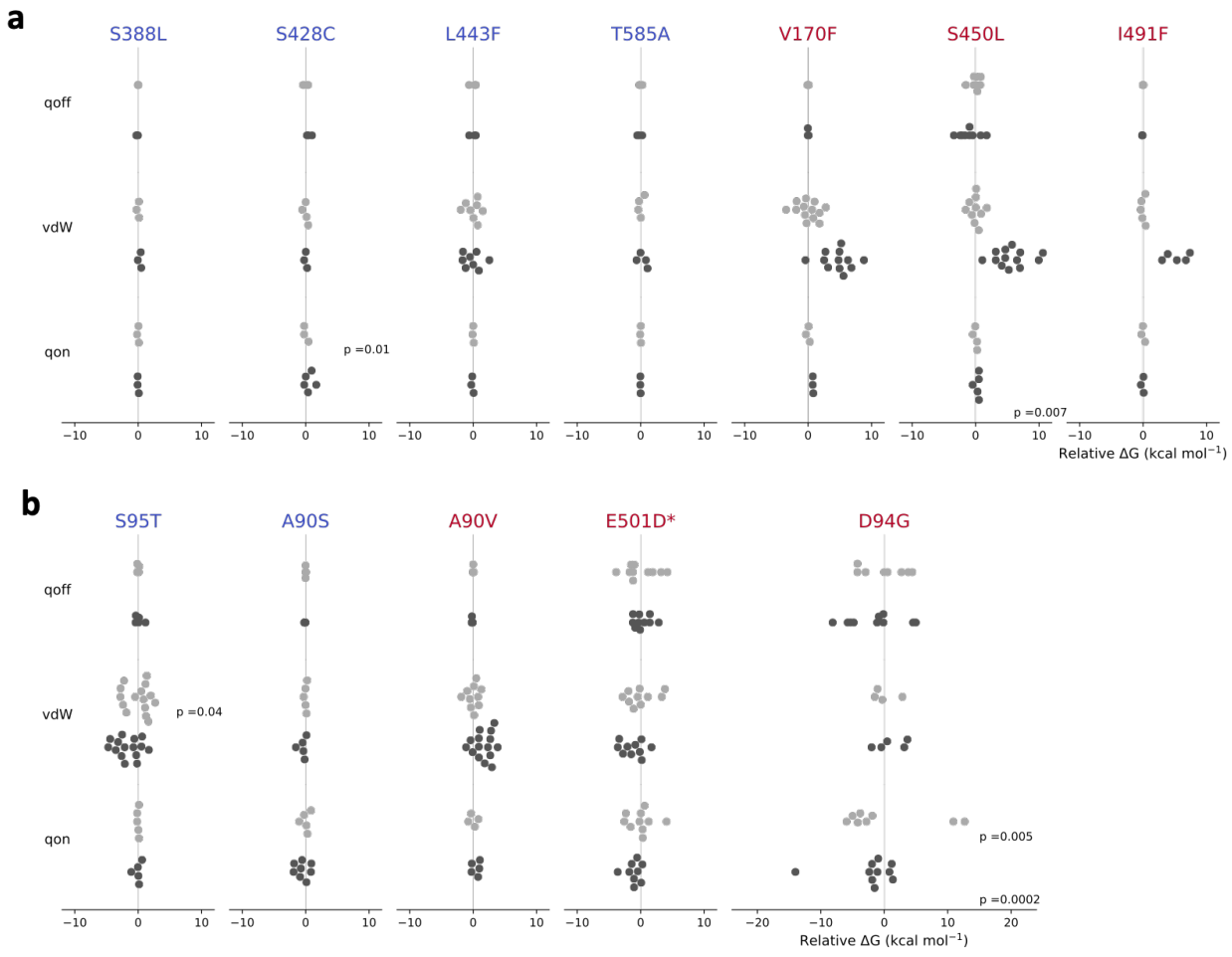

Figure 5. Swarm plots of individual results from apo (light grey) and drug bound (dark grey) alchemical free energy calculations for mutations in the RNA polymerase (a) and DNA gyrase (b). All results are normalized to the mean of the calculations for the apo leg for each qoff, vdW or qon transition for each mutation. p-values from Shapiro Wilks test are displayed for each transition showing evidence of non-normality in the repeated calculations, transitions where no p-value is shown indicates there was no evidence of non-normality in the data ($p > 0.05$). An asterisk (*) indicates a *gyrB* mutation.

By starting each simulation from a different structural seed and discarding the first half of the alchemical free energy simulations and then applying statistics to the resulting values of ΔG we are assuming that they are *independent*. If true, then one would also expect the values to be normally distributed which would appear to be the case for most sets of ΔG values (Figure 5). Applying the Shapiro-Wilks test of normality to the *rpoB* data confirms that, despite the small numbers of samples in some cases, the majority of ΔG values are indeed normally distributed with the exceptions of ΔG_{qon} for the apo leg of S428C and ΔG_{qon} for the drug bound leg of S450L. For two DNA gyrase mutations there was also evidence of non-normality in the ΔG_{vdW} for the apo leg of *gyrA* S95T and ΔG_{on} for both the apo and drug bound leg of *gyrA* D94G.

To test how far our simulations are from normality, we extended four apo and five drug-bound simulations underlying the most variable component (qon, Fig. 1) of the most complex mutation, *gyrA* D94G, by an order of magnitude (from 0.5 ns to 5 ns). As assessed by the Shapiro-Wilks, the resulting distributions of apo- and drug-bound free energies were indeed normal after 5 ns of simulation ($p = 0.92$ and $p = 0.16$) but the distribution of results for the repeated calculations, and therefore the error, remain large (Fig. S3).

DISCUSSION

We have shown how relative binding free energy (RBFE) techniques can be applied to large protein complexes to predict, with some success, the effect of individual protein mutations on the binding of an antibiotic, and thence whether resistance is conferred. When the size of the signal is large and the mutations do not involve significant changes in the electrical charge, as is the case for the *rpoB* mutations, one can successfully predict whether a mutation confers resistance to the antibiotic (in this case rifampicin). If the fold increase in minimum inhibitory concentration is small and/or there are significant charge changes, as is the case for most of the resistance conferring mutations in the DNA gyrase, then the estimated error of $\Delta\Delta G$ will likely be so large that no definite prediction can be made. In addition, the observed non-normality of the ΔG_{qon} free energy for *gyrA* D94G indicates that these values are also not independent: to solve this either the λ simulations would have to be extended or the equilibration simulations would need to be more numerous as well as longer.

Despite the focus on *resistance*, it is more useful to be able to accurately and reproducibly predict *susceptibility* since clinically that will lead to immediate action i.e. starting the patient on the appropriate treatment regimen. A prediction of resistance will likely result in the sample being sent for further testing, at which point any incorrect predictions (false positives) will be detected. Unfortunately, it may be more difficult to predict susceptibility than resistance using RBFE, and for *rpoB* only one susceptible mutation could be confidently predicted. If we assume that most susceptible mutations will not affect the binding affinity for the antibiotic, then they would have a $\Delta\Delta G$ of zero. The predicted $\Delta\Delta G$ of such mutations would hence require the estimated error to be

at least less than the value of the ECOFF (for *rpoB* and DNA gyrase 1.2 and 0.9 kcal/mol, respectively) to make a confident susceptible prediction. The magnitude of error for the mutations in this study was greater than the relevant ECOFF in all but one case (*rpoB* S388L, Table 1). It is likely that the error could be reduced by running a greater number of repeats, however some mutations can result in a small increase in MIC but not enough to confer resistance (as susceptibility can be defined as any MIC up to the ECOFF), and in such cases even a lower level of error (± 0.5 kcal/mol) may still prove insufficient for prediction.

Whilst alchemical binding free energy calculations therefore can play a role in predicting antibiotic resistance, the method currently works best when the target protein is small and the magnitude of the change in the binding free energy large, as is the case for *S. aureus* DHFR and trimethoprim[17]. For this system it has also been shown that it is possible to reduce the length of the simulations yet further but still maintain an accurate qualitative prediction[16]. Taking all this together, we appear to have probed the limits (for now at least) of using RBFE methods to predict antibiotic resistance *de novo*. Interestingly, unlike the majority of other applications of RBFE, one can tolerate large, estimated errors since we are ultimately only interested in the final binary classification of resistant or susceptible. A second and related application for RBFE is reducing the likelihood of a lead compound developing resistance by providing information during the development process of the likely mutations that could confer resistance and we hope to explore this in future work.

There are several shortcomings with our approach. We have assumed that resistance arises by reducing how well the antibiotic binds; this will not always be true. Secondly, our predictions

depend on the accuracy of the molecular forcefields that describe the interatomic interactions. Finally, we assume that the conformations used to seed each calculation are independent of one another and/or that the λ simulations are long enough to allow the initial state to be 'forgotten'. Given we chose to use very short λ simulations the latter is almost certainly not true and whilst the majority of our calculated ΔG values appear to be normally distributed, some are not which is concerning. One would expect to have to run 4x the number of simulations to reduce the estimated error to half its original value if the simulations are independent. This makes simulations of these size prohibitively computationally intensive at the time of writing.

It is not in doubt that how the structure and dynamics of a protein change upon mutation contains valuable information that can, in theory, be used to predict whether individual mutations confer antibiotic resistance. An alternative route, which is much less computationally intensive, is to train machine learning models using structural and chemical input features. This is the focus of future work and ultimately machine learning and RBFE/MD approaches may not only complement one another but also form part of a larger toolkit that helps us to tackle antimicrobial resistance by improving diagnosis.

ASSOCIATED CONTENT

Supporting Information. Figures S1-S3 are available in the Supporting Information, along with two CSV files; one for the RNAP and one for the DNAG. Each CSV contains a list of all the individual alchemical free energy transitions and their errors allowing Figure 4 and thence Figure 3 to be reproduced.

AUTHOR INFORMATION

Corresponding Author

* philip.fowler@ndm.ox.ac.uk, @philipwfowler

Author Contributions

AEB and PWF designed the study, setup, ran and analysed the simulations and wrote the manuscript.

Funding Sources

This study is funded by the National Institute for Health Research (NIHR) Health Protection Research Unit in Healthcare Associated Infections and Antimicrobial Resistance, a partnership between Public Health England and the University of Oxford. The research was also funded/supported by the National Institute for Health Research (NIHR) Oxford Biomedical Research Centre (BRC). The computational aspects of this research were supported by the Wellcome Trust Core Award Grant Number 203141/Z/16/Z and the NIHR Oxford BRC. Access to the ARCHER supercomputer was provided through CompBioMed, an EU H2020 Centre of Excellence project, and the UK High-End Computing Consortium for Biomolecular Simulation (HECBioSim, EP/R029407/1) which is supported by the EPSRC. AEB is funded by an NDM Prize

Studentship from the Oxford Medical Research Council Doctoral Training Partnership and the Nuffield Department of Clinical Medicine.

ACKNOWLEDGMENTS

We thank Prof. Ann Sarah Walker for her support. For the purpose of open access, the author has applied a CC BY public copyright license to any Author Accepted Manuscript version arising from this submission. The views expressed are those of the author(s) and not necessarily those of the NHS, the NIHR or the Department of Health.

ABBREVIATIONS

RNAP RNA polymerase, DNAG DNA gyrase, RIF rifampicin, MXF moxifloxacin, RBFE relative binding free energy, MDR TB multidrug resistant tuberculosis, RRDR rifampicin resistance determining region, QRDR quinolone resistance determining region, MD molecular dynamics, vdW van der Waals, MIC minimum inhibitory concentration, ECOFF epidemiological cutoff value.

REFERENCES

1. World Health Organization (WHO), Rapid Communication: Key changes to treatment of multidrug- and rifampicin-resistant tuberculosis (MDR/RR-TB) **2018**.
2. World Health Organization (WHO), Catalogue of mutations in Mycobacterium tuberculosis complex and their association with drug resistance. **2021,** *License: CC BY-NC-SA 3.0 IGO*.
3. Walker, T. M. a. M., Paolo and Köser, Claudio U. and Fowler, Philip William and Knaggs, Jeff and Iqbal, Zamin and Hunt, Martin and Chindelevitch, Leonid and Farhat, Maha and Cirillo, daniela and Comas, Iñaki and Posey, James E. and Omar, Shaheed Vally and Peto, Timothy E. A. and Suresh, Anita and Uplekar, Swapna and Laurent, Sacha and Colman, Rebecca and Nathanson, Carl-Michael and Zignol, Matteo and Walker, Ann Sarah and Consortium, The CRyPTIC and Consortium, The Seq&Treat and Crook, Derrick W. and Ismail, Nazir and Rodwell, Timothy C.,, The 2021 WHO Catalogue of Mycobacterium Tuberculosis Complex Mutations Associated with Drug Resistance: A New Global Standard for Molecular Diagnostics. *Preprints with The Lancet* **2021**.
4. Brankin, A.; Malone, K. M.; Barilar, I.; Battaglia, S.; Borroni, E.; Brandao, A. P.; Cabibbe, A. M.; Carter, J.; Cirillo, D. M.; Claxton, P.; Clifton, D. A.; Cohen, T.; Coronel, J.;

Crook, D. W.; Dreyer, V.; Earle, S. G.; Escuyer, V.; Ferrazoli, L.; Fowler, P. W.; Gao, G. F.; Gardy, J.; Gharbia, S.; Ghisi, K. T.; Ghodousi, A.; Cruz, A. L. G.; Grandjean, L.; Grazian, C.; Groenheit, R.; Guthrie, J. L.; He, W.; Hoffmann, H.; Hoosdally, S. J.; Hunt, M.; Iqbal, Z.; Ismail, N. A.; Jarrett, L.; Joseph, L.; Jou, R.; Kambli, P.; Khot, R.; Knaggs, J.; Koch, A.; Kohlerschmidt, D.; Kouchaki, S.; Lachapelle, A. S.; Lalvani, A.; Lapierre, S. G.; Laurenson, I. F.; Letcher, B.; Lin, W.-H.; Liu, C.; Liu, D.; Mandal, A.; Mansjö, M.; Matias, D.; Meintjes, G.; de Freitas Mendes, F.; Merker, M.; Mihalic, M.; Millard, J.; Miotto, P.; Mistry, N.; Moore, D.; Musser, K. A.; Ngcamu, D.; Nhung, H. N.; Niemann, S.; Nilgiriwala, K. S.; Nimmo, C.; Okozi, N.; Oliveira, R. S.; Omar, S. V.; Paton, N.; Peto, T. E.; Pinhata, J. M. W.; Plesnik, S.; Puyen, Z. M.; Rabodoarivelo, M. S.; Rakotosamimanana, N.; Rancoita, P. M.; Rathod, P.; Robinson, E.; Rodger, G.; Rodrigues, C.; Rodwell, T. C.; Roohi, A.; Santos-Lazaro, D.; Shah, S.; Kohl, T. A.; Smith, G.; Solano, W.; Spitaleri, A.; Supply, P.; Surve, U.; Tahseen, S.; Thuong, N. T. T.; Thwaites, G.; Todt, K.; Trovato, A.; Utpatel, C.; Van Rie, A.; Vijay, S.; Walker, T. M.; Sarah Walker, A.; Warren, R.; Werngren, J.; Wijkander, M.; Wilkinson, R. J.; Wilson, D. J.; Wintringer, P.; Xiao, Y.-X.; Yang, Y.; Yanlin, Z.; Yao, S.-Y.; Zhu, B., A data compendium of Mycobacterium tuberculosis antibiotic resistance. *bioRxiv* **2021**, 2021.09.14.460274.

5. The CRyPTIC Consortium; Allix-Beguec, C.; Arandjelovic, I.; Bi, L.; Beckert, P.; Bonnet, M.; Bradley, P.; Cabibbe, A. M.; Cancino-Munoz, I.; Caulfield, M. J.; Chaiprasert, A.; Cirillo, D. M.; Clifton, D. A.; Comas, I.; Crook, D. W.; De Filippo, M. R.; de Neeling, H.; Diel, R.; Drobniewski, F. A.; Faksri, K.; Farhat, M. R.; Fleming, J.; Fowler, P.; Fowler, T. A.; Gao, Q.; Gardy, J.; Gascoyne-Binzi, D.; Gibertoni-Cruz, A. L.; Gil-Brusola, A.; Golubchik, T.; Gonzalo, X.; Grandjean, L.; He, G.; Guthrie, J. L.; Hoosdally, S.; Hunt, M.; Iqbal, Z.; Ismail, N.; Johnston, J.; Khanzada, F. M.; Khor, C. C.; Kohl, T. A.; Kong, C.; Lipworth, S.; Liu, Q.; Maphalala, G.; Martinez, E.; Mathys, V.; Merker, M.; Miotto, P.; Mistry, N.; Moore, D. A. J.; Murray, M.; Niemann, S.; Omar, S. V.; Ong, R. T.; Peto, T. E. A.; Posey, J. E.; Prammananan, T.; Pym, A.; Rodrigues, C.; Rodrigues, M.; Rodwell, T.; Rossolini, G. M.; Sanchez Padilla, E.; Schito, M.; Shen, X.; Shendure, J.; Sintchenko, V.; Sloutsky, A.; Smith, E. G.; Snyder, M.; Soetaert, K.; Starks, A. M.; Supply, P.; Suriyapol, P.; Tahseen, S.; Tang, P.; Teo, Y. Y.; Thuong, T. N. T.; Thwaites, G.; Tortoli, E.; van Soolingen, D.; Walker, A. S.; Walker, T. M.; Wilcox, M.; Wilson, D. J.; Wyllie, D.; Yang, Y.; Zhang, H.; Zhao, Y.; Zhu, B., Prediction of Susceptibility to First-Line Tuberculosis Drugs by DNA Sequencing. *N Engl J Med* **2018,** *379* (15), 1403-1415.

6. Boehme, C. C.; Nabeta, P.; Hillemann, D.; Nicol, M. P.; Shenai, S.; Krapp, F.; Allen, J.; Tahirli, R.; Blakemore, R.; Rustomjee, R.; Milovic, A.; Jones, M.; O'Brien, S. M.; Persing, D. H.; Ruesch-Gerdes, S.; Gotuzzo, E.; Rodrigues, C.; Alland, D.; Perkins, M. D., Rapid molecular detection of tuberculosis and rifampin resistance. *N Engl J Med* **2010,** *363* (11), 1005-15.

7. World Health Organization (WHO). WHO policy statement: Automated real-time nucleic acid amplification technology for rapid and simultaneous detection of tuberculosis and rifampicin resistance: Xpert MTB/RIF system 2011. http://whqlibdoc.who.int/publications/2011/9789241501545_eng.pdf (accessed 7/24/2014).

8. Sanchez-Padilla, E.; Merker, M.; Beckert, P.; Jochims, F.; Dlamini, T.; Kahn, P.; Bonnet, M.; Niemann, S., Detection of drug-resistant tuberculosis by Xpert MTB/RIF in Swaziland. *N Engl J Med* **2015,** *372* (12), 1181-2.

9. Farhat, M. R.; Jacobson, K. R.; Franke, M. F.; Kaur, D.; Sloutsky, A.; Mitnick, C. D.; Murray, M., Gyrase Mutations Are Associated with Variable Levels of Fluoroquinolone Resistance in Mycobacterium tuberculosis. *J Clin Microbiol* **2016,** *54* (3), 727-33.
10. Miotto, P.; Tessema, B.; Tagliani, E.; Chindelevitch, L.; Starks, A. M.; Emerson, C.; Hanna, D.; Kim, P. S.; Liwski, R.; Zignol, M.; Gilpin, C.; Niemann, S.; Denkinger, C. M.; Fleming, J.; Warren, R. M.; Crook, D.; Posey, J.; Gagneux, S.; Hoffner, S.; Rodrigues, C.; Comas, I.; Engelthaler, D. M.; Murray, M.; Alland, D.; Rigouts, L.; Lange, C.; Dheda, K.; Hasan, R.; Ranganathan, U. D. K.; McNerney, R.; Ezewudo, M.; Cirillo, D. M.; Schito, M.; Koser, C. U.; Rodwell, T. C., A standardised method for interpreting the association between mutations and phenotypic drug resistance in Mycobacterium tuberculosis. *Eur Respir J* **2017,** *50* (6).
11. Walker, T. M.; Kohl, T. A.; Omar, S. V.; Hedge, J.; Del Ojo Elias, C.; Bradley, P.; Iqbal, Z.; Feuerriegel, S.; Niehaus, K. E.; Wilson, D. J.; Clifton, D. A.; Kapatai, G.; Ip, C. L. C.; Bowden, R.; Drobniewski, F. A.; Allix-Beguec, C.; Gaudin, C.; Parkhill, J.; Diel, R.; Supply, P.; Crook, D. W.; Smith, E. G.; Walker, A. S.; Ismail, N.; Niemann, S.; Peto, T. E. A.; Modernizing Medical Microbiology Informatics, G., Whole-genome sequencing for prediction of Mycobacterium tuberculosis drug susceptibility and resistance: a retrospective cohort study. *Lancet Infect Dis* **2015,** *15* (10), 1193-1202.
12. The CRyPTIC Consortium, J. J. C., Quantitative measurement of antibiotic resistance in Mycobacterium tuberculosis reveals genetic determinants of resistance and susceptibility in a target gene approach. *bioRxiv* **2021**.
13. Takiff, H. E.; Salazar, L.; Guerrero, C.; Philipp, W.; Huang, W. M.; Kreiswirth, B.; Cole, S. T.; Jacobs, W. R., Jr.; Telenti, A., Cloning and nucleotide sequence of Mycobacterium tuberculosis gyrA and gyrB genes and detection of quinolone resistance mutations. *Antimicrobial agents and chemotherapy* **1994,** *38* (4), 773-780.
14. Ajileye, A.; Alvarez, N.; Merker, M.; Walker, T. M.; Akter, S.; Brown, K.; Moradigaravand, D.; Schon, T.; Andres, S.; Schleusener, V.; Omar, S. V.; Coll, F.; Huang, H.; Diel, R.; Ismail, N.; Parkhill, J.; de Jong, B. C.; Peto, T. E.; Crook, D. W.; Niemann, S.; Robledo, J.; Smith, E. G.; Peacock, S. J.; Koser, C. U., Some Synonymous and Nonsynonymous gyrA Mutations in Mycobacterium tuberculosis Lead to Systematic False-Positive Fluoroquinolone Resistance Results with the Hain GenoType MTBDRsl Assays. *Antimicrob Agents Chemother* **2017,** *61* (4).
15. Pantel, A.; Petrella, S.; Veziris, N.; Brossier, F.; Bastian, S.; Jarlier, V.; Mayer, C.; Aubry, A., Extending the definition of the GyrB quinolone resistance-determining region in Mycobacterium tuberculosis DNA gyrase for assessing fluoroquinolone resistance in M. tuberculosis. *Antimicrob Agents Chemother* **2012,** *56* (4), 1990-6.
16. Fowler, P. W., How quickly can we predict trimethoprim resistance using alchemical free energy methods? *Interface Focus* **2020,** *10* (6).
17. Fowler, P. W.; Cole, K.; Gordon, N. C.; Kearns, A. M.; Llewelyn, M. J.; Peto, T. E. A.; Crook, D. W.; Walker, A. S., Robust Prediction of Resistance to Trimethoprim in Staphylococcus aureus. *Cell Chem Biol* **2018,** *25* (3), 339-349 e4.
18. Lin, W.; Mandal, S.; Degen, D.; Liu, Y.; Ebright, Y. W.; Li, S.; Feng, Y.; Zhang, Y.; Mandal, S.; Jiang, Y.; Liu, S.; Gigliotti, M.; Talaue, M.; Connell, N.; Das, K.; Arnold, E.; Ebright, R. H., Structural Basis of Mycobacterium tuberculosis Transcription and Transcription Inhibition. *Mol Cell* **2017,** *66* (2), 169-179 e8.

19. Blower, T. R.; Williamson, B. H.; Kerns, R. J.; Berger, J. M., Crystal structure and stability of gyrase-fluoroquinolone cleaved complexes from Mycobacterium tuberculosis. *Proc Natl Acad Sci U S A* **2016,** *113* (7), 1706-13.
20. Fiser, A.; Sali, A., ModLoop: automated modeling of loops in protein structures. *Bioinformatics* **2003,** *19* (18), 2500-1.
21. Lindorff-Larsen, K.; Piana, S.; Palmo, K.; Maragakis, P.; Klepeis, J. L.; Dror, R. O.; Shaw, D. E., Improved side-chain torsion potentials for the Amber ff99SB protein force field. *Proteins* **2010,** *78* (8), 1950-8.
22. Mark James Abraham, T. M., Roland Schulz, Szilárd Páll, Jeremy C. Smith, Berk Hess, Erik Lindahl, GROMACS: High performance molecular simulations through multi-level parallelism from laptops to supercomputers. *SoftwareX* **2015,** *1-2*, 19-25.
23. Hess, B.; Bekker, H.; Berendsen, H. J. C.; Fraaije, J. G. E. M., LINCS: A linear constraint solver for molecular simulations. *Journal of Computational Chemistry* **1997,** *18* (12), 1463-1472.
24. Gapsys, V.; Michielssens, S.; Seeliger, D.; de Groot, B. L., pmx: Automated protein structure and topology generation for alchemical perturbations. *J Comput Chem* **2015,** *36* (5), 348-54.
25. Jefferys, E.; Sands, Z. A.; Shi, J.; Sansom, M. S.; Fowler, P. W., Alchembed: A Computational Method for Incorporating Multiple Proteins into Complex Lipid Geometries. *J Chem Theory Comput* **2015,** *11* (6), 2743-2754.
26. Mey, A. S. J. S., Allen, B. K., Bruce McDonald, H. E., Chodera, J. D., Hahn, D. F., Kuhn, M., Michel, J., Mobley, D. L., Naden, L. N., Prasad, S., Rizzi, A., Scheen, J., Shirts, M. R., Tresadern, G., & Xu, H, Best Practices for Alchemical Free Energy Calculations [Article v1.0]. *Living Journal of Computational Molecular Science* **2020,** *2* (1), 18378.
27. World Health Organization (WHO), Technical report on critical concentrations for drug susceptibility testing of isoniazid and the rifamycins (rifampicin, rifabutin and rifapentine). **2021**.
28. The CRyPTIC Consortium, Epidemiological cutoff values for a 96-well broth microdilution plate for high-throughput research antibiotic susceptibility testing of M. tuberculosis. *medRxiv* **2021**.